RSC Advances

ROYAL SOCIETY OF CHEMISTRY

www.rsc.org/advances

Journal Name

ARTICLE

Design and characterization of gadolinium infused theranostic liposomes

Received 00th January 20xx,
Accepted 00th January 20xx

DOI: 10.1039/x0xx00000x

www.rsc.org/

Arunkumar Pitchaimani[a,b,c] Tuyen Duong Thanh Nguyen[a,b] Hongwang Wang[a], Stefan H. Bossmann[a], Santosh Aryal[a,b*]

Multifunctional theranostic gadolinium infused liposomes containing the chemotherapeutic drug, Doxorubicin (DOX), in its core are designed as potential candidates for diagnosis and therapy of various cancers. In these theranostic liposomes, Gd^{3+} ions are chelated by the macrocyclic chelator 1,4,7,10-tetraazacyclododecane-1,4,7,10-tetraacetic acid, which is covalently linked to the hydrophilic head moiety of the phospholipid. Therefore, the Gd^{3+} labels are an integral part of the lipid bilayer of liposomal construct. The physical properties of the Gd-infused liposomes were characterized including drug loading, drug release kinetics, cellular consequences, and T_1 weighted magnetic properties. The theranostic liposome exhibits uniform size distribution (hydrodynamic size of 150 ±10 nm) and a high drug loading efficiency with sustained drug release characteristics. Due to stable Gd^{3+} in their lipid bilayers, the theranostic liposomes displayed an enhanced r_1 relaxivity of 12.3$mM^{-1}s^{-1}$ at 14.1T, which is three times higher than that of currently used Gd-based clinical agent (Magnivest®: 4.1$mM^{-1}s^{-1}$, 1.4T). Moreover, cellular uptake studies revealed that these theranostic liposomes exhibit higher structural integrities inside B16-F10 melanoma cells. It shows uniform intracellular distribution throughout the cells. In-vitro cytotoxicity revealed that Gd-infused liposomes have excellent biocompatibility without significant cytotoxicity, whereas they showed higher cellular toxicity when loaded with DOX against B16-F10. The observed toxicity was equivalent to the same concentration of free DOX. With regard to the ongoing development in theranostic water-dispersible nanoformulations, the current formulation where Gd^{3+} ions are encapsulated by a macrocyclic chelator and covalently tethered to the hydrophilic head moiety of a lipid, is rather promising and holds great promise.

1. Introduction

Design and development of theranostic nanoparticles with multimodal imaging ability have gained much interest in recent years.[1–3] Among different nanoparticles, biocompatible liposomes and polymeric nanoparticles are well known for their multifunctional versatilities, which include enhanced drug loading efficiency of both hydrophilic and hydrophobic drugs, facile surface chemistry, straightforward size selection during synthesis, and minimizing off-target toxicity.[4–6] Particularly, surface modification flexibility of liposomes due to the functional groups present in the head moiety of the phospholipids allows various functional molecules to be attached covalently, thereby producing a highly stable surface membrane construct when formulated in the form of a liposome. Various drug formulations of liposomes are already in clinical trials and some of them are approved by FDA for clinical use and biomedical applications, which include cancer therapy.[7,8] On the other hand, magnetic resonance imaging (MRI) is an imaging modality that provides high spatial resolution, while avoiding the use of ionizing radiation. The low risk to patients makes it an appropriate and increasingly popular tool for clinical diagnosis. Therefore, merging liposomal delivery system with MRI capabilities would significantly improve the therapeutic outcome.[9–12]

Liposomes can be designed as a multifunctional theranostic nanoparticle system by encapsulating both chemotherapeutic drugs and image-guiding contrast agents.[13–15] Several experimental strategies have been formulated to develop theranostic liposomes by incorporating both chemotherapeutic drugs and various imaging contrast agents.[16,17] Although core loaded liposomes deliver both the chemotherapeutic and the MRI contrast agents together, they have several disadvantages like delayed contrast agent efficacy of MRI agents like Gadolinium (Gd), and toxicity related to Gd-based contrast agents. Retention of Gd is known to have serious consequences including the incurable and potentially life-

[a] Department of Chemistry, Kansas State University, Manhattan, KS 66506
[b] Nanotechnology Innovation Center of Kansas State (NICKS), Kansas State University, Manhattan, KS 66506
[c] Department of Anatomy and Physiology, Kansas State University, Manhattan, KS 66506.
* Corresponding author: Dr. Santosh Aryal, Email: saryal@ksu.edu.
Electronic Supplementary Information (ESI) available: [details of any supplementary information available should be included here]. See DOI: 10.1039/x0xx00000x

threatening disease known as Nephrogenic Systemic Fibrosis (NSF).[18–20]

The first approved contrast agent, Gd-DTPA (gadopentetate dimeglumine, Magnevist®) appeared in 1988 and several other compounds, such as Gd-BOPTA (gadobenate dimeglumine, Multihance®) and Gd-EOB-DTPA (gadoxetic acid disodium, sold as Primovist® in Europe, Eovist® in USA) are currently available in the US.[21–24] Chemically, these compounds exhibit three similar features: they all contain Gd^{3+}, an 8-coordinate ligand binding to Gd^{3+}, and a single water molecule coordination site to Gd^{3+}. The multidentate ligand is required for safety, because it encapsulated Gd^{3+} with high thermodynamic stability and kinetic inertness.[25] The high magnetic moment of the Gd^{3+} ion and the presence of a rapidly exchanging coordinated water molecule are essential to provide contrast.[26] However, current Gd^{3+}-based commercial agents have inefficient contrast enhancement capabilities due to their low relaxivity. In addition, these commercialized contrast agents are extracellular fluid (ECF) agents. Upon injection, ECF agents quickly and freely distribute to extracellular spaces within mammalian bodies. The average terminal half-life for blood elimination for all these compounds is about 1.5h, when administered to human subjects with normal renal function.[27] Those agents are therefore limited to targeting sites, where they can be expected to accumulate in high concentrations, such as in the blood stream and kidneys.[28] Recent studies have been focused on developing theranostic liposomes with chemotherapeutic drugs and MRI contrast agents. For example, liposomes loaded with Doxorubicin (DOX) and magnetic resonance imaging (MRI) agent Gadolinium show combined therapeutic effect with image guided clinical efficiency.[28–31] Several studies have been formulated to develop gadolinium based liposomes for combined chemotherapy and bio-imaging.[9,11,26,32] Most of these study designs are limited to two categories, (I) liposomes encapsulating both drugs and gadolinium contrast agent in the aqueous core of a vesicle, which decreases the clinical efficacy of drugs and lowers magnetic relaxivity due to hindering water affinity as therapeutic payload is also present in the core, and (II) post surface modification with gadolinium by using ligand molecules, which raises concerns about the drug loading efficiency and stability of both Gd^{3+} ions and the entire liposomes in-vivo.[12,29,32–34]

In the present study, we have formulated a theranostic liposomal drug delivery system featuring the surface attachment of Gd^{3+} to DSPE (distearoylphosphatidylethanolamine) chelated with the macrocycle DOTA (1,4,7,10-tetraazacyclododecane-1,4,7,10-tetraacetic acid) and core-loaded chemotherapeutic drug DOX. In the current formulation, Gd^{3+} is chelated into the macrocyclic chelate (DOTA) attached covalently to the head moiety of a phospholipid, which makes it easier to infuse into the bilayer of a stable liposomal formulation. Three different formulations of Gd-labeled liposomes were prepared by altering the ratio of Gd^{3+} and phospholipids. The physical properties of the Gd-infused theranostic liposomes were characterized along with cellular uptake studies and in-vitro toxicity analysis.

2. Experimental

2.1 Chemicals & reagents

Gadolinium(III) chloride was purchased from Alfa Aesar (Ward Hill, MA), Cholesterol was purchased from Fisher, and all other lipids like 1,2-distearoyl-sn-glycero-3-phosphoethanolamine (DSPE), 1,2-dioctadecanoyl-sn-glycero-3-phospho-(1'-rac-glycerol) (sodium salt) (DSPG), 1,2-distearoyl-sn-glycero-3-phosphoethanolamine-N-[succinyl(polyethylene glycol) -2000] (ammonium salt) (DSPG-PEG-Succinyl), (1,2-distearoyl-sn-glycero-3-phospho ethanolamine-N-(7-nitro-2-1,3-benzoxadiazol-4-yl) (ammonium salt) (DSPE-NBD) were purchased from Avanti Polar Lipid Inc. (Alabaster, AL, USA). N-Hydroxysuccimidyl ester activated 1,4,7,10-tetraazacyclododecane-1,4,7,10-tetraacetic acid (DOTA-NHS) was purchased from Macrocyclics. The Mouse Melanoma Cell line B16-F10 (ATCC® CRL-6475™) was maintained in Dulbecco's modified Eagle's medium (DMEM) supplemented with 10% (v/v) fetal bovine serum (FBS) and penicillin/streptomycin (100µg/mL) at 37°C in 5% CO_2 environment. All other chemicals and solvents were purchased from Sigma-Aldrich (Milwaukee, WI, USA) and used as received.

2.2 Synthesis of Gd-DOTA-DSPE

The Gd^{3+} ion chelating lipid was synthesized in a two-step preparation method as previously described.[35] In brief, 100mg of DSPE was hydrated with PBS for 5h and then 100mg of DOTA-NHS was added. The reaction mixture was continuously stirred for 6h. The mixture was then purified by dialysis (Mw Cutoff: 3K) in distilled water for 24h. The resulting DSPE-DOTA was further treated with Gadolinium (III) chloride (molar ratio 1:2), dissolved in acetate buffer (pH=6.0) at 50°C for 24h. After incubation, the Gd-DOTA-DSPE was further purified by dialysis. The samples were lyophilized to obtain a dry powder. The percentage yield of the gadolinium concentration in the reaction mixture was analysed by using Inductively Coupled Plasma Mass spectrometry (ICP-MS, Perkin Elmer, NEXion 350X). The resulting yield was 85%.

2.3 Preparation of Gd-Infused liposomes

Gd-infused liposomes were prepared using DSPG:Gd-DOTA-DSPE:DSPG-PEG-Succinyl:cholesterol in the molar ratio of 33:35:18:14 using the lipid hydration and extrusion technique. In brief, defined molar concentrations of the lipids dissolved in chloroform were mixed together in a clean glass vials and dried under vacuum for 4 to 6h. The dried lipid film was hydrated with 1X Phosphate buffer saline (pH=7.4) and incubated at 50°C for 30 min and then mixed vigorously by means of sonication to obtain a clear dispersion of lipids. The liposomal dispersions were further extruded by using a Millipore membrane filters with different pore sizes (1µm, 400nm, and 100nm). Different formulations of Gd-infused liposomes were prepared by altering the molar ratio of Gd-

DOTA-DSPE and DSPG-PEG-Succinyl to 1:2, 1:1 and 2:1. The extruded infused liposomes were stored at 4°C for further use.

2.4 Preparation of Gd-infused theranostic liposomes

Drug loaded Gd^{3+} surface labelled theranostic liposomes were prepared by loading the chemotherapeutic drug, doxorubicin (DOX), into the core of the liposome. In a typical experiment, the lipid films were directly hydrated with a defined amount of DOX (5%, 10% and 20% of total lipid weight), suspended in 1X PBS, followed by the extrusion procedure at 50°C, as described above. Free DOX was removed by Sephadex G-50 column purification (GE Healthcare). The amount of encapsulated DOX and the resulting encapsulation efficiency was determined spectrophotometrically.

2.5 Characterization of liposomes

The hydrodynamic size and zeta potential of the bare and DOX encapsulated infused liposomes were characterized by using Dynamic light scattering analysis (Malvern Nano ZSP, UK). The anatomical structure of the liposomes was studied using Transmission electron microscope (FEI Technai G2 spirit BioTWIN). The amount of Gd incorporated into the liposomes was determined in Inductively Coupled Plasma Mass Spectrometry (ICP-MS, Perkin Elmer, NEXion 350X). For ICP-MS, the infused liposome samples were digested with 1.0ml of concentrated HNO3. After chemical digestion, 100µl of the sample was diluted with 5ml of 2%HNO3 and analysed by means of ICP-MS.

2.6 DOX and Gd release kinetics

The cumulative drug and Gd release from the DOX loaded Gd-infused liposomes was assessed under physiological condition at 37°C. In brief, DOX loaded infused liposomes (25µg/mL, 1mL) were placed in a dialysis bag membrane (Mw. Cutoff=12-14kDa) and dialyzed against 250mL of PBS (pH=7.4). At constant stirring (100 rpm), 500µL of sample was taken at predetermined time intervals. The amount of released DOX was quantified by measuring the DOX fluorescence with the excitation and emission wavelength of 490nm and 580nm. As control experiment, 25ug/mL of Free DOX was placed in a dialysis bag and processed under the same condition. For studying the Gd release, the samples were digested in concentrated HNO_3 and the analyte were dissolved in 2% HNO_3 for ICP-MS analysis.

2.7 Relaxometric analysis

The MRI relaxivity of Gd-infused theranostic liposomes was performed using a 14.1T NMR system (Bruker Avance III, WB, 600MHz NMR-MRI). The longitudinal relaxation time of different formulations of the Gd-infused theranostics (Gd-1, Gd-2 and Gd-3) in aqueous solution at equivalent Gd^{3+} concentration (10ug/mL) was determined using an inversion recovery pulse sequence. The longitudinal relaxivity (r_1) was determined from the T_1 relaxation time and the concentration of Gd^{3+} (in mM) and the corresponding T_1 weighted magnetic resonance phantom images were also recorded using a turbo spin echo sequence with TR=1500ms, TE=5.50ms and slice thickness= 1mm.

2.8 Cellular uptake studies

The cellular uptake and intracellular distribution of Gd-infused theranostics were tested using mouse melanoma cell line, B16-F10. Herein, the fluorescent due to DOX was taken an advantage to visualize the cellular uptake of theranostic liposome. In order to verify the structure integrity of the liposome during cellular internalization, the liposomes were further labelled with DSPE-NBD in their lipid bilayers and the co-localization of red (due to DOX) and green fluorescence (due to NBD) was studied. In brief, cells were seeded in a Poly-D-lysine coated 8 chamber slide placed at a density of 50,000cells/well. The confluent monolayer of cells was treated with 5µg/mL of NBD-labelled Gd-infused theranostic liposomes and incubated for 3h. After incubation, cells were washed twice with PBS (pH 7.4) and stained with DAPI for 10min. Cells were fixed and observed directly in a Confocal Laser Scanning Microscope (Carl Zeiss, LSM-700).

2.9 In-vitro cytotoxicity assay

The in-vitro cytotoxicity of DOX loaded liposomes and free DOX was investigated using a Mouse melanoma cell line B16-F10 using MTT assay. In brief, 2 x 10^4 cells per well in DMEM medium were seeded in a 96-well plate and incubated for 24h. After incubation, the media were replaced with different DOX concentration of DOX loaded Gd-infused liposomes and free DOX (4, 8.6, 13, 17, 21, 26 and 34 µM). The cells were incubated for 24h. Control cells were also maintained without any drug treatment (n=6). After 24h of drug exposure, the medium was replaced with fresh medium and continuously incubated for additional 48h, maintaining a total incubation time of 72h. After the completion of incubation, MTT was added to each well and further incubated for 3h according to the manufacturer recommendation. The insoluble formazan crystals were solubilized using DMSO and their absorbance was recorded at 570 nm using a microplate reader (BioTek, Synergy H1 hybrid reader).

3. Result and discussion

Liposomes are widely used as carriers for MRI contrast agents (CAs), in order to improve their efficiency by enhancing MRI signals, which are often based on the design that lead to be more favourable environment for proton exchange with water.[9,11,12,32,36] Three categories of liposomal MRI CAs have been described most frequently in the literatures.[10,37] The first is entrapping typical paramagnetic agents, such as Gd·DTPA, in the inner hydrophilic core of liposomes, the second type being entrapped at the free floating PEGylated corona, and the third is entrapped in between the lipid bilayer. However, in the first system, it cannot be ignored that encapsulation into the aqueous core of liposome may reduce the relaxivity of the paramagnetic agents because of the limited access to exchange with water as the core is also occupied by therapeutic payload.[9] Although in the second system, the PEGylated

corona has water accessibility, only a few molecules of Gd^{3+} chelators can be conjugated, which in turn masks the end functional moiety of PEG, reducing the liposomal stability. On the other hand, in the third system, in which the contrast agents are physically entrapped in the lipid bilayer in higher amount, the stability of liposomes is always a concern. Herein the Gd^{3+} ions are chelated to the macrocyclic chelator and covalently conjugated with the hydrophilic head moiety

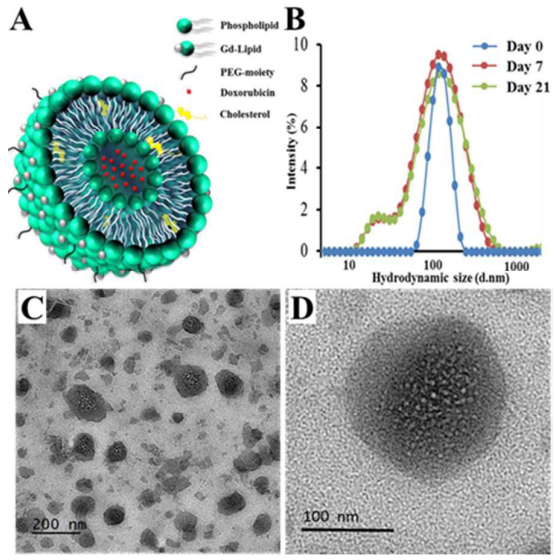

Fig. 1 Physiochemical properties and the anatomical structure of Gadolinium infused liposomes. (A) Schematic illustration of Gd-infused gadolinium liposomes. (B) Hydrodynamic size distribution showing stability of DOX loaded infused liposome stored at 4°C over 21 days of study. (C) Transmission electron micrograph of well dispersed DOX loaded infused liposome, (D) High magnification TEM of single liposome with encapsulated DOX crystals in its core. TEM was acquired after staining liposomes with uranyl acetate.

of a lipid, making them an integral part of lipid bilayer, results in the stabilization of the contrast agents with highly accessible surface area to load these agents. In addition, these lipid bilayers constantly exchange water via diffusion to maintain the lipid dynamics and colloidal stability. Under such conditions, proton exchange with neighbouring water is highly favourable.

3.1 Physiochemical characterization of Gd-infused liposomes

In this study, Gd-infused liposomes using DSPG:Gd-lipid:DSPG-PEG-Succinyl:cholesterol in the molar ratio of 33:35:18:14 were prepared by using the thin-film hydration method.[38,39] Fig. 1A shows a schematic illustration of surface labelled Gd^{3+} ions on the liposomes. Phospholipid conjugated Gd (Gd-lipid) was prepared via a simple convenient method as described in earlier reports.[35,40] With the purified Gd-lipid, three formulations of Gd-infused liposomes were prepared as described in Table 1. As each formulation has different molar concentrations of Gd-lipid/DSPG composition (1:1, 1:2, 2:1), the Gd-infused theranostic liposomes were prepared using DOX as a model drug. In this experiment, the calculated DOX concentration (10% by lipid weight) was passively loaded into the different liposomal formulations by directly adding DOX as hydrating agent during lipid film hydration procedure of the liposome preparation. The resulting liposomes were purified by Sephadex column to remove free drug. The average hydrodynamic diameters of the three formulations of liposomes were found to be 113±9 nm, 156±3 nm, and 120±8 nm, respectively. The observed narrow polydispersity index (PDI ranges from 0.09-0.25) is implying their good dispersion stability in an optimal size range for tumor targeting by the enhanced permeability and retention (EPR) effect. The zeta potential of these liposomes were found to be -56,-53 and -39 mV, respectively. The negative zeta potential is due to the surface carboxylate groups at the end moiety of the PEG corona. The prepared liposomal formulations were stable for prolong period of time, as demonstrated in Fig. 1B. After day 7, a small shoulder (less than 2% by intensity) peak appeared in the DLS spectrum, possibly due to the release of DOX over time, which could create inhomogeneity in the colloidal solution due to the release of DOX. The Gd^{3+} ion content of the three formulations were found to be 46±2, 74±1 and 109±2 µg/mL for Gd-1, Gd-2, and Gd-3, respectively. The higher Gd^{3+} content of the formulation Gd-3, is due to the higher Gd-Lipid/DSPG ratio. Among all formulations, Gd-2 exhibits higher monodispersity than Gd-1 or Gd-3. This is possibly due to the equivalent molar concentration of Gd-lipid and DSPG that causes the uniform distribution of all types of phospholipids throughout the liposomal membranes. Therefore, this formulation was selected as the choice for drug release and cytotoxicity measurements. With these assurances of the hydrodynamic size of infused liposomes, Gd-2 was subjected for its structural integrity using TEM measurement. As shown in Fig. 1C, the spherical assembly of liposomes with inner core containing crystallites of DOX was clearly visible. The multi-distributed spherical entities of various size in TEM micrographs (Figure 1C) is due to the fact that liposomes are aqueous nanodroplet with their interior having water which gets removed during the

Table 1 Dynamic light scattering analysis of various formulations of Gd-infused liposomes and its Gd^{3+} content

Formulations	Gd-Lipid:DSPG (moles)	Hydrodynamic Size (d.nm)	Zeta potential (mV)	Gd^{3+} Content (µg/mL)
Gd- 1	1:2	113.17±9.22	-56.6±1.2	45.6±2.3

Gd- 2	1:1	156±3.68	-52.9±1.8	74.15±0.8
Gd- 3	2:1	120.27±7.43	-39.2±3.4	109.12±2.2

sample preparation and especially in the high vacuum within the TEM. Moreover, the higher magnification image of infused liposome clearly shows that the crystallites of DOX are embedded into the core of the liposome (Fig. 1D).

3.2 Drug loading and release study

Next we examined the maximum drug encapsulation efficiency of Gd-2 formulations by increasing the initial input concentration of DOX to 5, 10 and 20% (by total lipid weight). The calculated initial concentrations of DOX were loaded into Gd-2 with the Gd-Lipid/DSPG ratio of 1:1(Gd-2). Fig. 2A shows the DOX encapsulation efficiency of these liposomes at varying DOX concentrations. By varying the initial DOX feeding concentration (5, 10 and 20% of total lipid weight), the maximum encapsulation efficiency (EE%) of the Gd-Liposome (Gd-2) was found to be ~55%. Furthermore, the higher DOX input in Gd-infused Liposomes resulted in lesser encapsulation efficiency and affected the physiological stability of the liposomes. Using the DOX loaded liposomes, the in-vitro drug release was investigated at pH=7.4 in phosphate buffer saline (PBS). A cumulative drug release study was performed using 12-14 kDa molecular cut-off dialysis bags. An optimization experiment was performed using an aqueous solution of free DOX placed in the dialysis tubing. The results indicate that most of the free drug was released within the period of 6h. This confirms the optimized condition for the drug release study. At pH=7.4, DOX loaded Gd-infused liposomes exhibit sustained drug release characteristics over a 96h time period at 37°C (Fig. 2 B). After 6h, nearly 30% of the drug was released. This is in agreement with our liposome stability test results, in which a small intensity peak appeared (centred at 30 nm), presumably due to the release of the drug and subsequent aggregation. At 37°C, only 10% of Gd^{3+} was released from the liposomes, indicating the structural stability of Gd^{3+} in the optimized liposomes (Fig. 2B inset).

3.3 Magnetic properties

As discussed above, among three types of Gd-based MRI CAs, the formulation proposed herein contains the Gd^{3+} as an integral part of lipid bilayer in the liposome, which provides greater access to proton exchange with water, as compared to that of previously reported formulations.[9,11,32,37] Since Gd-based CAs enhance T_1 -weighted MRI, it is critical to determine the magnetic efficiency in which the paramagnetic liposomes shorten the T_1 relaxation time of water in three formulations. T_1 relaxation efficiency was conveniently expressed as molar relaxivity, r_1, in unit $mM^{-1}s^{-1}$, which

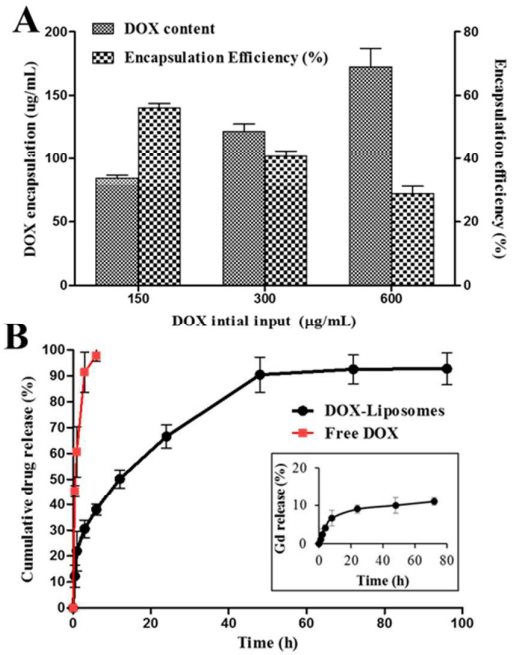

was determined from the dependence of the measured T_1 relaxation rate on the Gd^{3+} ion concentration. Fig. 3 shows the magnetic resonance properties of three formulations of Gd-labeled theranostic liposomes (Gd-1, Gd-2 and Gd-3). At equivalent concentrations of gadolinium, Gd-2 exhibits higher T_1 relaxivity showing 12.3±1.5 $mM^{-1}s^{-1}$ measured at 14.1 T, whereas other formulations Gd-1 and Gd-2 show 8.5±1.0 $mM^{-1}s^{-1}$ and 7.3±1.8 $mM^{-1}s^{-1}$, respectively. The higher T_1 relaxivity of Gd-2 is probably due to the equivalent surface distribution of Gd^{3+}

Fig. 2 Payload encapsulation and release studies. (A) DOX encapsulation efficiency of infused liposome with different initial input concentration of DOX (100, 300 and 600μg/mL). (B) Cumulative DOX release profile of free DOX and DOX loaded infused

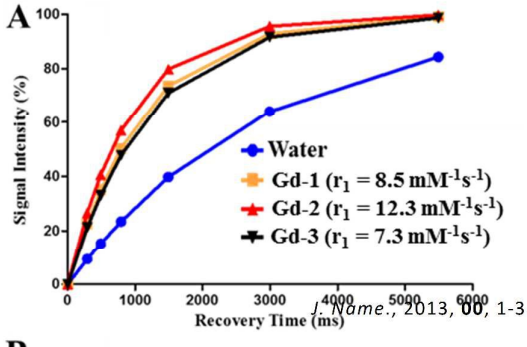

liposome at physiological condition (pH 7.4 at 37 °C), inset show the stability of Gd-infused liposomes over time at physiological condition.

Fig. 3 Magnetic properties of Gd-infused liposomes. (A) T_1 recovery curve of three formulations of Gd-infused Liposomes showing r_1= 8.5 (Gd-1), 12.3(Gd-2) and 7.3 (Gd-3) $mM^{-1}s^{-1}$. (B) Contrast phantoms of infused theranostic liposomes acquired at 14.1T

Table 2 Commercially available gadolinium based contrast agents for magnetic resonance imaging.

S.No	Gd based Contrast agents	Generic Name	Structural type	r1 ($mM^{-1}S^{-1}$)	Tesla	References
1	Magnevist®	Gadopentetate dimeglumine	Linear ionic	4.1	1.5T	[22]
2	Optimark®	Gadoversetamide	Linear non-ionic	4.7	1.5T	[23]
3	Primovist®	Gadoxetic acid disodium salt	Linear ionic	6.9	1.5T	[22]
4	Multihance®	Gadobenate dimeglumine	Linear ionic	6.7	1.5T	[24]
5	Prohance®	Gadoteridol	Macrocyclic non-ionic	3.1	3T	[41]
6	Dotarem®	Gadoteric acid	Macrocyclic ionic	3.6	1.5T	[22]
7	Vasovist®	Gadofosveset trisodium	Linear ionic	8.9	7T	[41]
8	Gadovist®	(Gadobutrol)	Macrocyclic non-ionic	5.2	1.5T	[23]
9	Omniscan®	(Gadodiamide)	Linear non-ionic	4.3	1.5T	[22]
10	Omniscan®	(Gadodiamide)	Linear non-ionic	4.6	14.1T	[42]
11	Gd-labelled	Gd-2	Gd-Infused liposome	12.3	14.1T	In this research

ions and DSPG exposed to bulk water molecules.[29,43] The presence of DSPG with its terminal glycol moiety has a tendency to capture water molecules via hydrogen bonding. This effect is ultimately increasing the water concentration at the vicinity of Gd-lipid. In a similar system, Gd-DTPA was attached to BSA when incorporated into the bilayer. It has shown the r_1 relaxivity of 5.2 $mM^{-1}s^{-1}$ measured at 7.0 T.[12] When introducing paramagnetic Gd·DOTA·BSA into the liposomal system, the resulting r_1 value was 4.10 ±0.34 $mM^{-1}s^{-1}$ measured at 4.7 T.[18] Similarly, DNA surface modified Gd nanoparticle was synthesized in a water/oil microemulsion, which exhibits r1 relaxivity of 0.2 $mM^{-1}s^{-1}$ measured at 14.1 T.[42] However, the current formulation showed 12.3±1.5 $mM^{-1}s^{-1}$ at 14.1T, thus confirming the feasibility of increasing the relaxivity of MRI CAs by incorporating Gd^{3+} at the bilayer of the liposome. It is clearly visible, when comparing the currently used Gd-based contrast agents with our formulation (Table 2), that our theranostic liposomes exhibit a higher relaxivity. Based on the observed enhancement in relaxivity, we further studied the contrast efficiency of the liposomes. The corresponding phantom images are presented in Fig. 3B.

3.4 Cellular studies of theranostic liposomes

After understanding the magnetic properties of the Gd-infused liposomes, we have studied the cellular uptake, which is a key factor to decide the therapeutic efficiency of any nanoformulation.[11,32] The cellular uptake efficiency of the DOX loaded theranostic liposomes was investigated using B16-F10 cells under confocal laser scanning microscopy with some modification in Gd-infused liposome preparation in order to labelled with NBD dye in its membrane. In general, liposomes are well known for their fusogenic properties with cellular membranes.[44–47] In order to confirm whether the theranostic liposomes can penetrate cellular membrane completely, or whether they release their DOX content in the cellular vicinity, we prepared theranostic liposomes with (1,2-distearoyl-sn-glycero-3-phospho ethanolamine-N-(7-nitro-2-1,3-benzoxadiazol-4-yl) (ammonium salt) (DSPE-NBD) in their formulation. NBD is a known green fluorescent dye showing excitation and emission wavelength at 470nm and 525nm, respectively. Fig. 4A shows the cellular uptake efficiency of DOX loaded infused liposomes, which were incubated with B16-F10 cells for 3h at 37°C. The higher cellular uptake with uniform intracellular distribution of DOX loaded liposomes were observed along with perinuclear localization in B16-F10 cells. The colocalization of signals due to NBD as an integral part of lipid bilayer and DOX as a core of liposome, clearly shows that the complete liposomes penetrated the cellular membrane along with DOX in its original form. This in turn, also supports our stability data and passivation due to PEG. The colocalization of red and green fluorescent is clearly visible by the formation to the yellow color. Moreover, Fig. 4B shows Z-stack confocal images, which confirms the intracellular co-localization of both DOX and NBD liposomes, thereby approving the structural stability of liposome into the cell.

Furthermore, the in-vitro cytotoxicity of the DOX loaded liposomes was tested in B16-F10 cells using the MTT assay. B16-F10 cells were treated with different concentration of DOX loaded liposomes and free DOX (4, 8.6, 13, 17, 21, 26, 34uM) for 24h at 37°C. Control cells were also maintained with equivalent concentration of blank liposome (without DOX). The results showed that the cell viability is

Journal Name

ARTICLE

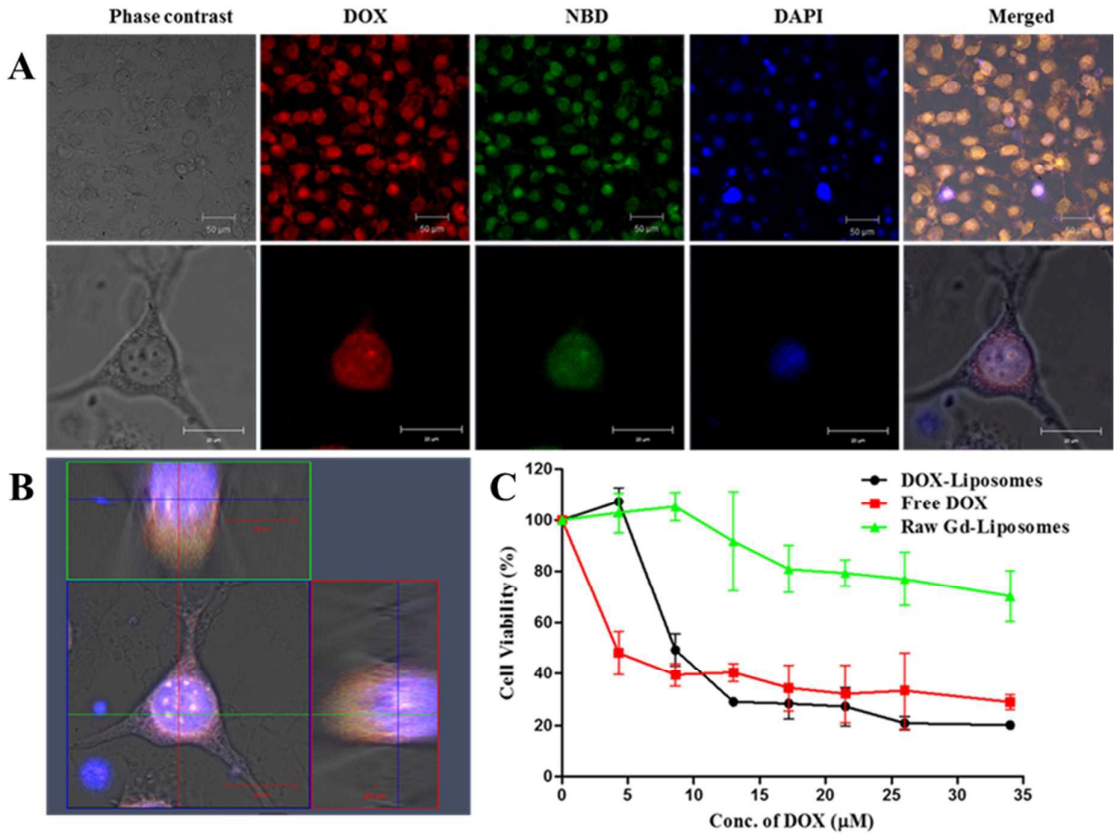

Fig. 4 Cellular uptake and in vitro cytotoxicity of Gd-infused theranostic liposome. (A) Confocal laser scanning microscopic images of B16-F10 cells incubated with 5ug/mL of DOX loaded infused liposome for 3h. Left to right column shows phase contrast, DOX fluorescence, NBD fluorescence, DAPI fluorescence, and merged fields. Top and bottom images represents magnification at 10X and 20X. (B) Z-stack of single B16-F10 cells incubated with DOX loaded Gd-infused liposome labelled with DSPE-NBD as a part of lipid bilayer showing intracellular distribution of particles throughout the cytoplasm and perinuclear regions. (C) In vitro cytotoxicity of different concentration of DOX loaded liposome and Free DOX in B16-F10 cell line after 24h treatment. Gd-infused liposome without DOX with equivalent liposome concentration was taken as a control.

not affected by the tested concentration of blank liposomes, suggesting the excellent biocompatibility role of Gd-lipid in our formulation. In contrast, both DOX loaded liposome and free DOX exhibit dose dependent cytotoxicity in B16-F10 cells. At lower concentration, free DOX showed higher cytotoxicity than DOX loaded liposomes, whereas at higher concentration both free DOX and DOX loaded theranostic liposomes shows equivalent cytotoxic effects suggesting the chemotherapeutic potential of DOX loaded infused liposomes against mouse melanoma cells.

4 Conclusion

In conclusion, this study demonstrated the theranostic potential of surface infused Gadolinium liposomes with excellent biocompatibility and enhanced T_1 relaxivity at higher magnetic strength, 14.1 T. Along with typical drug encapsulation and release characteristics, the Gd-infused liposomes proposed herein exhibits higher cellular uptake with uniform intracellular distribution without disrupting the structure of liposome. The in-vitro cytotoxicity assay against B16-F10 mouse melanoma cells further suggests their potential in therapeutic application. Moreover, the wide diversity of lipid structures and ease of chemical modification of the lipid head moieties will enable multi-functionality such as attachment of targeting ligands, cell penetrating peptides, and

fluorescent dyes, with which cell binding, uptake, and disease integration would be more efficient. This presents an opportunity in the design of tailored liposomal theranostic agents for imaging and simultaneous treatment of numerous solid tumors.

Acknowledgements

The authors acknowledge the support from the Department of Chemistry and the Nanotechnology Innovative Center of Kansas State (NICKS), Kansas State University, Manhattan, Kansas (KSU). Stefan Bossmann acknowledges support from the National Science Foundation (NSF-1128570 and NSF-1337438). The authors also thank the Confocal Core supported by CVM-KSU.

Notes and references

1 G. S. R. Raju, L. Benton, E. Pavitra and J. S. Yu, *Chem. Commun.*, 2015, **51**, 13248–13259.
2 M. D. K. Glasgow and M. B. Chougule, *J. Biomed. Nanotechnol.*, 2015, **11**, 1859–1898.
3 F. Jia, X. Liu, L. Li, S. Mallapragada, B. Narasimhan and Q. Wang, *J. Control. Release Off. J. Control. Release Soc.*, 2013, **172**, 1020–1034.
4 J. O. Eloy, M. Claro de Souza, R. Petrilli, J. P. A. Barcellos, R. J. Lee and J. M. Marchetti, *Colloids Surf. B Biointerfaces*, 2014, **123**, 345–363.
5 J. Nicolas, S. Mura, D. Brambilla, N. Mackiewicz and P. Couvreur, *Chem. Soc. Rev.*, 2013, **42**, 1147–1235.
6 R. A. Siegel, *J. Control. Release Off. J. Control. Release Soc.*, 2014, **190**, 337–351.
7 C. M. Dawidczyk, C. Kim, J. H. Park, L. M. Russell, K. H. Lee, M. G. Pomper and P. C. Searson, *J. Control. Release Off. J. Control. Release Soc.*, 2014, **187**, 133–144.
8 Y. Barenholz, *J. Control. Release Off. J. Control. Release Soc.*, 2012, **160**, 117–134.
9 N. Ding, Y. Lu, R. J. Lee, C. Yang, L. Huang, J. Liu and G. Xiang, *Int. J. Nanomedicine*, 2011, **6**, 2513–2520.
10 N. Kamaly and A. D. Miller, *Int. J. Mol. Sci.*, 2010, **11**, 1759–1776.
11 N. Kamaly, T. Kalber, M. Thanou, J. D. Bell and A. D. Miller, *Bioconjug. Chem.*, 2009, **20**, 648–655.
12 W. J. M. Mulder, G. J. Strijkers, A. W. Griffioen, L. van Bloois, G. Molema, G. Storm, G. A. Koning and K. Nicolay, *Bioconjug. Chem.*, 2004, **15**, 799–806.
13 W. Yuan, R. Kuai, R. Ran, L. Fu, Y. Yang, Y. Qin, Y. Liu, J. Tang, H. Fu, Q. Zhang, M. Yuan, Z. Zhang, F. Gao and Q. He, *J. Biomed. Nanotechnol.*, 2014, **10**, 1563–1573.
14 E. Salvati, F. Re, S. Sesana, I. Cambianica, G. Sancini, M. Masserini and M. Gregori, *Int. J. Nanomedicine*, 2013, **8**, 1749–1758.
15 D. Almeda, B. Wang and D. T. Auguste, *Biomaterials*, 2015, **41**, 37–44.
16 S. Rizzitelli, P. Giustetto, J. C. Cutrin, D. Delli Castelli, C. Boffa, M. Ruzza, V. Menchise, F. Molinari, S. Aime and E. Terreno, *J. Control. Release Off. J. Control. Release Soc.*, 2015, **202**, 21–30.
17 C.-J. Wen, L.-W. Zhang, S. A. Al-Suwayeh, T.-C. Yen and J.-Y. Fang, *Int. J. Nanomedicine*, 2012, **7**, 1599–1611.
18 J.-M. Idée, N. Fretellier, M. M. Thurnher, B. Bonnemain and C. Corot, *Ann. Pharm. Fr.*, 2015, **73**, 266–276.
19 R. Saito, M. T. Krauze, J. R. Bringas, C. Noble, T. R. McKnight, P. Jackson, M. F. Wendland, C. Mamot, D. C. Drummond, D. B. Kirpotin, K. Hong, M. S. Berger, J. W. Park and K. S. Bankiewicz, *Exp. Neurol.*, 2005, **196**, 381–389.
20 W. J. Chu, T. Simor and G. A. Elgavish, *NMR Biomed.*, 1997, **10**, 87–92.
21 M. A. Kirchin, G. P. Pirovano and A. Spinazzi, *Invest. Radiol.*, 1998, **33**, 798–809.
22 M. Rohrer, H. Bauer, J. Mintorovitch, M. Requardt and H.-J. Weinmann, *Invest. Radiol.*, 2005, **40**, 715–724.
23 Y. Shen, F. L. Goerner, C. Snyder, J. N. Morelli, D. Hao, D. Hu, X. Li and V. M. Runge, *Invest. Radiol.*, 2015, **50**, 330–338.
24 L. Johansson, M. A. Kirchin and H. Ahlström, *Acta Radiol. Stockh. Swed. 1987*, 2012, **53**, 1112–1117.
25 P. Caravan, J. J. Ellison, T. J. McMurry and R. B. Lauffer, *Chem. Rev.*, 1999, **99**, 2293–2352.
26 S. Aime and P. Caravan, *J. Magn. Reson. Imaging JMRI*, 2009, **30**, 1259–1267.
27 H. J. Weinmann, M. Laniado and W. Mützel, *Physiol. Chem. Phys. Med. NMR*, 1984, **16**, 167–172.
28 Q. Liu, H. Zhu, J. Qin, H. Dong and J. Du, *Biomacromolecules*, 2014, **15**, 1586–1592.
29 K. Na, S. A. Lee, S. H. Jung and B. C. Shin, *Colloids Surf. B Biointerfaces*, 2011, **84**, 82–87.
30 S. Erdogan and V. P. Torchilin, *Methods Mol. Biol. Clifton NJ*, 2010, **605**, 321–334.
31 S. Erdogan, Z. O. Medarova, A. Roby, A. Moore and V. P. Torchilin, *J. Magn. Reson. Imaging JMRI*, 2008, **27**, 574–580.
32 M. B. Kok, S. Hak, W. J. M. Mulder, D. W. J. van der Schaft, G. J. Strijkers and K. Nicolay, *Magn. Reson. Med.*, 2009, **61**, 1022–1032.
33 R. Saito, J. R. Bringas, T. R. McKnight, M. F. Wendland, C. Mamot, D. C. Drummond, D. B. Kirpotin, J. W. Park, M. S. Berger and K. S. Bankiewicz, *Cancer Res.*, 2004, **64**, 2572–2579.
34 K. Ghaghada, C. Hawley, K. Kawaji, A. Annapragada and S. Mukundan, *Acad. Radiol.*, 2008, **15**, 1259–1263.
35 S. Aryal, J. Key, C. Stigliano, J. S. Ananta, M. Zhong and P. Decuzzi, *Biomaterials*, 2013, **34**, 7725–7732.
36 N. Kamaly, T. Kalber, A. Ahmad, M. H. Oliver, P.-W. So, A. H. Herlihy, J. D. Bell, M. R. Jorgensen and A. D. Miller, *Bioconjug. Chem.*, 2008, **19**, 118–129.
37 W. J. M. Mulder, G. J. Strijkers, G. A. F. van Tilborg, A. W. Griffioen and K. Nicolay, *NMR Biomed.*, 2006, **19**, 142–164.
38 C. E. Smith, A. Shkumatov, S. G. Withers, B. Yang, J. F. Glockner, S. Misra, E. J. Roy, C.-H. Wong, S. C. Zimmerman and H. Kong, *ACS Nano*, 2013, **7**, 9599–9610.
39 C. Grange, S. Geninatti-Crich, G. Esposito, D. Alberti, L. Tei, B. Bussolati, S. Aime and G. Camussi, *Cancer Res.*, 2010, **70**, 2180–2190.
40 S. Li, B. Goins, L. Zhang and A. Bao, *Bioconjug. Chem.*, 2012, **23**, 1322–1332.
41 N. P. Blockley, L. Jiang, A. G. Gardener, C. N. Ludman, S. T. Francis and P. A. Gowland, *Magn. Reson. Med.*, 2008, **60**, 1313–1320.

42 M. F. Dumont, C. Baligand, Y. Li, E. S. Knowles, M. W. Meisel, G. A. Walter and D. R. Talham, *Bioconjug. Chem.*, 2012, **23**, 951–957.
43 M. de Smet, E. Heijman, S. Langereis, N. M. Hijnen and H. Grüll, *J. Control. Release Off. J. Control. Release Soc.*, 2011, **150**, 102–110.
44 J. Connor, M. B. Yatvin and L. Huang, *Proc. Natl. Acad. Sci. U. S. A.*, 1984, **81**, 1715–1718.
45 N. Düzgüneş, H. Faneca and M. C. Lima, *Methods Mol. Biol. Clifton NJ*, 2010, **606**, 209–232.
46 D. Pornpattananangkul, S. Olson, S. Aryal, M. Sartor, C.-M. Huang, K. Vecchio and L. Zhang, *ACS Nano*, 2010, **4**, 1935–1942.
47 K. W. Mok and P. R. Cullis, *Biophys. J.*, 1997, **73**, 2534–2545.